

Original Article

Flavonoid-Rich Extract of *Oldenlandia diffusa* (Willd.) Roxb. Inhibits Gastric Cancer by Activation of Caspase-Dependent Mitochondrial Apoptosis*

LING Jia-yin^{1,2}, WANG Qiu-lan^{1,2}, LIANG Hao-nan^{1,2}, LIU Qing-bo^{1,2}, YIN Dong-hong^{1,2}, and LIN Li^{3,4}

ABSTRACT **Objective:** To evaluate the apoptosis and cycle arrest effects of *Oldenlandia diffusa* flavonoids on human gastric cancer cells, determine the action mechanisms in association with the mitochondrial dependent signal transduction pathway that controls production of reactive oxygen species (ROS), and evaluate the pharmacodynamics of a mouse xenotransplantation model to provide a reference for the use of flavonoids in prevention and treatment of gastric cancer. **Methods:** Flavonoids were extracted by an enzymatic-ultrasonic assisted method and purified with D-101 resin. Bioactive components were characterized by high-performance liquid chromatography. Cell lines MKN-45, AGS, and GES-1 were treated with different concentrations of flavonoids (64, 96, 128, and 160 $\mu\text{g/mL}$). The effect of flavonoids on cell viability was evaluated by MTT method, and cell nuclear morphology was observed by Hoechst staining. The apoptosis rate and cell cycle phases were measured by flow cytometry, the production of ROS was detected by laser confocal microscope, the mitochondrial membrane potential (MMP) were observed by fluorescence microscope, and the expression of apoptotic proteins related to activation of mitochondrial pathway were measured by immunoblotting. MKN-45 cells were transplanted into BALB/c nude mice to establish a xenograft tumor model. Hematoxylin and eosin staining was used to reveal the subcutaneous tumor tissue. The tumor volume and tumor weight were measured, the expression levels of proliferation markers proliferating cell nuclear antigen (PCNA) and Ki-67 were detected by immunohistochemistry, and the expression levels of CA72-4 were measured by enzyme linked immunosorbent assay. **Results:** *Oldenlandia diffusa* flavonoids inhibited proliferation of MKN-45 and AGS human gastric cancer cells, arrested the cell cycle in G₁/S phase, induced accumulation of ROS in the process of apoptosis, and altered MMP. In addition, flavonoids increased Apaf-1, Cleaved-Caspase-3, and Bax, and decreased Cyclin A, Cdk2, Bcl-2, Pro-Caspase-9, and Mitochondrial Cytochrome C ($P < 0.05$). The MKN-45 cell mouse xenotransplantation model further clarified the growth inhibitory effect of flavonoids towards tumors. The expression levels of PCNA and Ki-67 decreased in each flavonoid dose group, the expression level of CA72-4 decreased ($P < 0.05$). **Conclusion:** Flavonoids derived from *Oldenlandia diffusa* can inhibit proliferation and induce apoptosis of human gastric cancer cells by activating the mitochondrial controlled signal transduction pathway.

KEYWORDS Chinese medicine, *Oldenlandia diffusa* flavonoids, gastric cancer, apoptosis, mitochondria

Gastric cancer is a common gastrointestinal tumor, ranking as the third leading cause of cancer-related death.⁽¹⁾ Each year, 990,000 people worldwide are diagnosed with gastric cancer. New cases and deaths in developing countries accounted for 71.15% and 75.84% of age-standardized morbidity, respectively.⁽²⁾ Reducing the incidence and mortality of gastric cancer is a significant public health problem. For patients with nonmetastatic early gastric cancer, surgery is the conventional treatment.⁽³⁾ The individualized treatment schemes recommended and implemented in different countries are different for patients with advanced gastric cancer. The overall prognosis of advanced gastric

©The Chinese Journal of Integrated Traditional and Western Medicine Press and Springer-Verlag GmbH Germany, part of Springer Nature 2022

*Supported by the Key Research and Development Program of Gansu Province (No. 21YF5FA131), the Innovation Fund of Gansu Universities (No. 2021A-084), and the Graduate Innovation Fund of Gansu University of Chinese Medicine (No. 2021CX49)

1. First School of Clinical Medicine, Gansu University of Chinese Medicine, Lanzhou (730000), China; 2. Gansu Provincial Hospital, Lanzhou (730000), China; 3. College of Pharmacy, Gansu University of Chinese Medicine, Lanzhou (730000), China; 4. Institute of Chinese (Tibetan) Medicine Resources, Gansu University of Chinese Medicine, Lanzhou (730000), China
 Correspondence to: Associate Prof. WANG Qiu-lan, E-mail: qiulwang@163.com

DOI: <https://doi.org/10.1007/s11655-022-3679-4>

cancer is not optimistic, and the 5-year survival rate is only 5%–20%.⁽⁴⁾

Multidrug resistance to chemotherapeutic drugs is a common phenomenon of tumors.⁽⁵⁾ Natural drugs used in Chinese medicine (CM) have low toxicity and high safety. Compared with single-component drugs used in Western medicine, CM compounds may circumvent drug resistance. Therefore, the development of CM compounds has essential value. *Oldenlandia diffusa* is the most common traditional Chinese antitumor medicine.⁽⁶⁾ The herb has a variety of biological characteristics and pharmacological activities. Extracts include mainly iridoid compounds, flavonoids, anthraquinones, phenolic acids and their derivatives, sterols, volatile oil compounds, alkaloids, polysaccharides, cyclic peptides, and coumarins. These components have anti-inflammatory, antioxidant, immunoregulation, and neuroprotection activities.⁽⁷⁻⁹⁾ *Oldenlandia diffusa* extract can inhibit the growth of tumors such as glioblastoma,⁽¹⁰⁾ prostate cancer,⁽¹¹⁾ cervical cancer,⁽¹²⁾ liver cancer,⁽¹³⁾ and lung cancer,⁽¹⁴⁾ and such extracts promote tumor cell apoptosis. Previously, we found that *Oldenlandia diffusa* flavonoids inhibited proliferation of BGC-823 gastric cancer cells and promoted their apoptosis.⁽¹⁵⁾ However, the mechanism of flavonoid-induced apoptosis has not been identified. Understanding the mechanism of induced apoptosis is important for intervention and treatment of tumor diseases.

We extracted *Oldenlandia diffusa* flavonoids by an enzymatic-ultrasonic method and purified the material with a D-101 resin.^(16,17) In this study, *in vitro* and *in vivo* experiments were used to identify the molecular mechanism and target of flavonoid inhibition of tumors.

METHODS

Plant Material

Dried whole grass *Oldenlandia diffusa* (Willd.) Roxb. (Origin: Yuzhou City, Henan Province), belonging to the *Rubiaceae* family, was identified by Prof. LIN Li, School of Pharmacy, Gansu University of Chinese Medicine. Some samples were stored for reference in herbarium of the School of Pharmacy. Rutin was purchased from National Institutes for Food and Drug Control (No. MUST-14101410).

Enzymatic-Ultrasonic Extraction of Flavonoids

After crushing, *Oldenlandia diffusa* was screened with 65 mesh pharmacopoeia (5.0 g). Cellulase, papain,

and pectinase (1:1:1) were added to the sample and mixed with 60% ethanol. After evaporation and concentration in a water bath for 90 min, the solid-liquid ratio was 1:20 (g/mL). Then the sample was subjected to ultrasonic extraction for 30 min, inactivation in a boiling water bath for 5 min, vacuum filtration, and made to a constant volume with 70% ethanol. The best combination of factors was tested 3 times.

Purification of Flavonoids with Adsorption Resin

A sample (0.32 g) of dry extract was mixed with distilled water. The loading mass concentration was 2.18 mg/mL. The natural extract (80.0 mL) was wet-loaded into a glass column (2 cm × 30 cm), which was wet-packed with D-101 (5.0 g) resin and eluted with 50.0 mL of 80% ethanol (flow rate 4.0 mL/min). All kinetic experiments were performed at ambient temperature.

Measurement of Flavonoids

The flavonoids were measured as rutin equivalents. To draw the standard curve, we measured 0, 0.5, 1.0, 1.5, 2, 2.5, 3, and 3.5 mL of rutin standard solution (0.1 mg/mL), added 4 mL of 1% AlCl₃ solution, and made the volume to 10 mL with 95% ethanol. After 15 min, the absorbance was measured with a UV-vis spectrometer (Shimadzu, Japan). The flavonoid solution was prepared and analyzed according to the above method. The content of flavonoid was calculated from the rutin standard curve.

Preparation of Flavonoid Solution

The purified flavonoids were prepared as a 160.00 μg/mL solution with RPMI-1640 (BI, Israel), filtered with 0.22 μm microporous membrane and stored at 4 °C.

Identification of Active Components in *Oldenlandia diffusa* Flavonoids

High-performance liquid chromatography (HPLC, Agilent HPLC1260, USA) with a SinoChromODS-AP (4.6 mm × 250 mm, 5 μm) column was used to analyze the flavonoid mixture. The mobile phase was methanol (A)-0.1% phosphoric acid solution (B), gradient elution (0–7 min, 40% A; 7–20 min, 45% A; 20–35 min, 55% A; 35–45 min, 75% A) with a column temperature as 35 °C. The volume flow was 1.0 mL/min, and the detection wavelength of the diode array detector was 280 nm. The standards were passed through a 0.45 μm filter before use. Methanol was chromatographically pure (Sigma, USA), and the purity of rutin (No. 20191501), quercetin (No. 20190701), kaempferol (No. 20181071), baicalin

(No. 20191081), and nobiletin (No. 20191105) was more than 98%.

Cell Culture

Human gastric cancer cell line MKN-45 (No. CL-0292) was provided by Prof. LI Hong-ling of Gansu Provincial Hospital. AGS cells were purchased from Wuhan Procell Life Science & Technology Co., Ltd., China (No. CL-0022). Human gastric mucosal cell line GES-1 (No. CL-0563) was provided by Prof. LIU Hong-bin of the 940th Hospital of Joint Logistics Support Force of People's Liberation Army. The cells were cultured in RPMI-1640 medium with 10% fetal bovine serum (GIBCO, USA) and 1% penicillin-streptomycin (Solarbio, China). The culture medium was replaced and supplemented for 2 days. The cells were subcultured at 80% confluence and cultured in a 37 °C, 5% CO₂ humidity incubator (Sanyo, Japan).

Methyl Thiazolyl Tetrazolium Cell Viability Assay

MKN-45, AGS and GES-1 in logarithmic growth phase were digested with trypsin, and the cell concentration was adjusted to 5.0×10^4 /mL. The cells were inoculated into 96-well plates (100 μ L/well), a set of 6 wells for each group, and transferred to an incubator for 24 h (5% CO₂, 37 °C). In the experimental group, total flavonoids to 64, 96, 128, 160 μ g/mL for 24, 48, and 72 h were added. Then, 20 μ L methyl thiazolyl tetrazolium (MTT) solution was added to each well and the plates were incubated for 4 h. The culture medium was discarded, 150 μ L dimethyl sulfoxide (DMSO) was added, and the plates were agitated for 10 min. Blank control (RPMI-1640, MTT, DMSO) and negative control (cell, RPMI-1640, MTT, DMSO) were prepared simultaneously. Optical density (OD) at 492 nm was measured using a microplate reader (Thermo Fisher, USA). Linear regression method was used to calculate the half inhibitory concentration (IC₅₀), with the formula cell viability (%) = [OD (experimental) – OD (blank)]/[OD (negative) – OD (blank)] \times 100%.

Effect of Flavonoids on Gastric Cancer Cell Nuclear Morphology

Hoechst 33342 staining was used to detect the morphological characteristics of the cell apoptosis induced by *Oldenlandia diffusa* flavonoids. MKN-45 and AGS cells (2.0×10^5 /mL) were grown to logarithmic phase in a 6-well plate for 24 h. Total flavonoids were added to 64, 96, 128, 160 μ g/mL for 48 h. The cells were fixed with 4% paraformaldehyde for 30 min and washed twice with phosphated buffered saline (PBS). We added 5 μ L

Hoechst staining solution (10 μ g/mL) to each well, and the plate was cooled in an ice-bath for 20 min. The nuclei of cells were observed with an inverted fluorescence microscope (Olympus BX51, Japan).

Apoptosis Detection

MKN-45 and AGS cells (1.0×10^6 /mL) in log phase were inoculated into 60-mm cell culture dishes and treated with 64, 96, 128, and 160 μ g/mL flavonoids for 48 h. RPMI-1640 medium was used as a vehicle control. Annexin V-FITC/PI double staining was used to measure apoptosis according to instructions from Yeasen Biotechnology Co., Ltd. (China). The cells were incubated at ambient temperature in the dark for 15 min, then subjected to flow cytometry (BD Biosciences, USA) to measure the number of apoptotic cells by Flowjo 10.7.1 (Tree Star, USA). Annexin V positive/PI negative indicated the percent of early apoptosis, and annexin V/PI double-positive showed the percent of late apoptosis.

Cell Cycle Analysis

MKN-45 and AGS cells (1.0×10^6 /mL) were treated with 64, 96, 128, and 160 μ g/mL flavonoids for 48 h. The cells were collected in 70% ethanol at 4 °C overnight. Pre-cooled PBS was used to wash and fix the cells once. The cells were stained with PI storage solution and RNase A solution at 37 °C in the dark for 30 min and filtered with 300 mesh nylon net. The samples were analyzed in a flow cytometer. Cellquest (BD Biosciences) was used to measure the DNA content in each stage of the cell cycle.

Effects of Flavonoids on Mitochondrial Membrane Potential

Mitochondrial membrane potential (MMP) was measured with the 1,1',3,3'-tetraethyl-5,5',6,6'-tetrachloroimidocarbocyanine iodide (JC-1) detection kit (Yeasen). The MKN-45 and AGS cells (5.0×10^4 /mL) were inoculated in 6-well plates and cultured for 24 h. They were treated with flavonoids at 64, 96, 128, and 160 μ g/mL or with RPMI-1640 medium for 48 h. The JC-1 staining solution was added and incubated at 37 °C for 20 min, and JC-1 staining buffer (1 \times) was used to wash twice for observation of membrane potential. The positive control carbonyl cyanide 3-chlorophenylhydrazone (50 μ mol/L) was set to observe the pretreated cells for 20 min. In the vehicle control, JC-1 dye was concentrated in the mitochondrial matrix and formed red fluorescent aggregates. After flavonoid treatment, the mitochondrial membrane depolarized to form a green fluorescent JC-1 monomer.

Image-pro Plus 6.0 software (Media Cybernetics, USA) were used to analyze the average optical density (AOD), and the mitochondrial depolarization level was expressed as red fluorescent AOD / green fluorescent AOD.

Measurement of Intracellular Reactive Oxygen Species

The reactive oxygen species (ROS) level produced by the gastric cancer cell lines treated with flavonoids was assessed by 2,7-dichlorofluorescein diacetate (DCFH-DA) staining. The DCFH-DA is cell-permeable and is hydrolyzed by nonspecific esterases and oxidized by intracellular peroxide to form DCF. The strength of DCF fluorescence is directly proportional to the amount of ROS. The generation of ROS in cells was measured with the fluorescent probe DCFH-DA in a kit (Solarbio). The MKN-45 and AGS cells (5.0×10^4 /mL) were inoculated on the cell climbing slides of 12-well plates, and the cells were grown to 80% confluence. The cells were treated with 64, 96, 128, and 160 μ g/mL flavonoids for 48 h. The culture medium was removed, 10 μ mol/L DCFH-DA was added and incubated at 37 °C for 30 min. The cells were washed twice with the RPMI-1640 culture medium, and the cell climbing slides were placed on the glass slides and observed by laser confocal microscope (Leica TCS SP8, Germany). Flavonoids and intervention of H₂O₂ (1 mmol/L) or N-acetyl-L-cysteine (NAC, 5 mmol/L) pretreatment were set in parallel. The excitation wavelength was 488 nm.

Immunoblotting Analysis

MKN-45 cells (1.0×10^6 /mL) was treated with 64, 96, 128, and 160 μ g/mL flavonoids and RPMI-1640 medium (vehicle control) for 48 h. The cells were lysed for 30 min with 1 mL RIPA buffer containing 10 μ L phenylmethanesulfonyl fluoride (Solarbio), and the protein concentration was measured by the bicinchoninic acid (BCA) method. A 4× loading buffer and sample were heated at 100 °C for 10 min at a ratio of 1:3. Sample loading quantity was 15 μ L on sodium dodecyl sulfate polyacrylamide gel electrophoresis (SDS-PAGE). The gel contents were transferred to a membrane which was probed with tris-buffered saline with Tween (TBST)-diluted rabbit anti-human Cyclin A (No. YT1167), Cdk2 (No. YT0832), and Apaf-1 (No. YT5378) monoclonal antibodies at 1:1000 (Immunoway, USA) and rabbit anti-human Caspase-9 (No. YT0662), Caspase-3 (No. YT0656), Bcl-2 (No. YT0470), and Bax (No. YT0455) monoclonal antibodies at 1:1500 (Immunoway, USA), incubated overnight at 4 °C. A Tubulin- β (No. YT4780)

monoclonal antibody was used to detect the protein as an internal reference. The probed membrane was incubated with secondary antibody at ambient temperature for 2 h, decolorized and washed with TBST 3 times. Chemiluminescence detection was performed. A ChemiDoc MP gel imaging system (Bio-Rad, USA) was used, and the development strip was analyzed by ImageLab image processing software.

Isolation and Detection of Mitochondrial Proteins

MKN-45 cells (1.0×10^6 /mL) were collected and resuspended in precooled reagent A of a mitochondrial separation kit (Yeasen) and incubated on ice for 15 min. The plasma membrane was disrupted by ultrasound. The lysate was centrifuged at $1000 \times g$ for 15 min. The supernatant was centrifuged at $12,000 \times g$ at 4 °C for 10 min to obtain mitochondria. Pre-cooled reagent B and reagent C solutions were added to the pellet, incubated at 4 °C for 15 min, and centrifuged at 10,000 r/min for 15 min. The BCA method was used to measure protein concentration of the supernatant. The release of Cytochrome C (No. GTX108585) was detected by immunoblotting. Rabbit anti-human Cytochrome C monoclonal antibody (GeneTex, USA) was diluted 1:800 with TBST. COX IV (No. GTX114330) was used as an internal reference protein (GeneTex).

Antitumor Effect of *Oldenlandia diffusa* Flavonoids in vivo

The animal experiment was approved by the Ethics Committee of the Animal Experiment Center of Gansu University of Chinese Medicine (No. 2021-226). Male BALB/c nude mice, 4–5-week-old, were purchased from Beijing SiPeiFu Biotechnology Co., Ltd. (China). Experiments were conducted in the SPF animal laboratory of Gansu University of Chinese Medicine. MKN-45 cells (9.0×10^6 /mL) were resuspended by PBS (100 μ L) and injected subcutaneously into the armpit to establish a mouse gastric cancer xenotransplantation model. When the tumor reached 200–300 mm³, the mice were treated with flavonoid at a high dose (200 mg·kg⁻¹·d⁻¹), medium dose (100 mg·kg⁻¹·d⁻¹), low dose (50 mg·kg⁻¹·d⁻¹), and blank control (0.9% normal saline, respectively). The drug was administered by gavage once every 2 days, a total of 10 times. The tumor volumes were observed daily, and the tumor sizes were measured with a caliper every 2 days ($n=6$). Tumor volume was calculated as [length (mm) × width square (mm²)]/2. Blood was collected after the tenth intragastric administration. Tumor weight were measured after abdominal anesthesia (ketamine

hydrochloride, 2 mL: 0.1 g; No. 1709291). The reference basis of gavage dose of flavonoid is reported.^(18,19)

Evaluation of Serological Indexes

Mouse serum samples were stored at -80°C . Serum CA72-4 were measured with an enzyme-linked immunosorbent assay kit (Mlbio, China); a standard was provided with the kit. Samples were diluted by a factor of 25, and 50 μL of the sample was added into each well. Then, 100 μL of enzyme-labeled reagent was added into each well. The plate was incubated 60 min at 37°C after closure. Next, the plate was rinsed 5 times with detergent 30 s each time, and 100 μL of color-developing agent was added. The plate incubated in the dark at 37°C for 15 min. The reaction was terminated. The OD values of each well of the enzyme-coated plate was measured at 450 nm in a plate reader (BIOTEK Cytation, Germany).

Hematoxylin and Eosin Staining and Immunohistochemistry

Sections (3 μm) of tumor tissue were fixed with 4% paraformaldehyde, dehydrated with an ethanol gradient, made transparent with xylene, and embedded in paraffin. Tumor cells and tumor necrosis areas were evaluated by hematoxylin and eosin staining. Immunohistochemistry was conducted according to the streptavidin-peroxidase method (ZSGB-BIO, China). Ethylene diamine tetraacetic acid antigen repair solution (pH=8.0) was heated at high temperature and high pressure for 3 min. Mouse anti-human proliferating cell nuclear antigen (PCNA) and Ki-67 monoclonal antibodies (ZSGB-BIO) were incubated with the sections overnight at 4°C . Biotin-labeled goat anti-mouse IgG was applied at ambient temperature for 15 min. The sections were incubated at ambient temperature for 15 min with horseradish peroxidase-labeled streptomyces ovalbumin working solution and finally DAB was developed. Nuclei with positive expression of PCNA (No. ZM-0213) and Ki-67 (No. ZM-0166) were brownish yellow or brown under an inverted microscope imaging system (Olympus DP27, Japan). Image Pro Plus 6.0 (Media Cybernetics, USA) was used to randomly analyze four regions AOD of each section.

Statistical Analysis

Experiments were repeated 3 times and shown as the means \pm standard deviation ($\bar{x} \pm s$). Statistical analysis was conducted with SPSS 25.0 software (IBM, Armonk, USA) and GraphPad Prism 8.0 software (GraphPad Software Inc., San Diego, USA). A rutin standard curve was constructed for a regression equation. The coefficients of determination (R^2) were

calculated to evaluate the goodness of fit of the regression model coefficient. For comparisons between groups of more than two unpaired values, a one-way analysis of variance (ANOVA) was used. If an ANOVA F value was significant, post-hoc comparisons were performed between groups. If data did not distribute normally, the Kruskal-Wallis H test was used to compare groups of more than two unpaired values. $P < 0.05$ was considered to indicate a statistically significant difference.

RESULTS

Content of Flavonoids in *Oldenlandia diffusa*

When the flavonoid content was 0.005–0.035 mg/mL, the regression equation was $Y = 28.718 \cdot X - 0.0119$ ($R^2 = 0.9995$), where Y , X and R^2 represented the OD values at 495 nm, flavonoid concentration (mg/mL), and determination coefficient, respectively. The average recovery was 96.64% ($n=3$). The average yield of flavonoid was 1.97%, the pure product accounted for 28.62% of the crude extract, and the purity was 57.5%.

Content of Active Components in Flavonoids

Figure 1 shows the content of rutin, quercetin, kaempferol, baicalein, and nobiletin in *Oldenlandia diffusa* flavonoids. The calibration curve showed a good linear relationship when rutin and kaempferol were 6–96 $\mu\text{g/mL}$ ($r=0.9997$), quercetin was 4.5–73 $\mu\text{g/mL}$ ($r=0.9996$), baicalein was 0.7–11.2 $\mu\text{g/mL}$ ($r=0.9999$), and nobiletin was 0.6–9.6 $\mu\text{g/mL}$ ($r=0.9998$). The regression equations of the 5 compounds are summarized in Appendix 1. Rutin, quercetin, kaempferol, baicalein and nobiletin accounted for 2.6%, 0.5%, 0.17%, 0.031%, and 0.018%, respectively, of the *Oldenlandia diffusa* flavonoids.

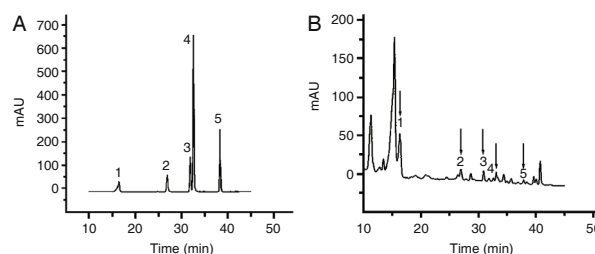


Figure 1. Bioactive Components in *Oldenlandia diffusa* Flavonoids

Notes: (A, B) HPLC chromatograms of reference substances and sample, respectively. 1. rutin; 2. quercetin; 3. kaempferol; 4. baicalein; 5. nobiletin. (C) The flavonoids use C6-C3-C6 as skeleton

Inhibitory Effect of Flavonoids on Growth of Human Gastric Cancer Cells

As shown in Figure 2, the flavonoids efficiently

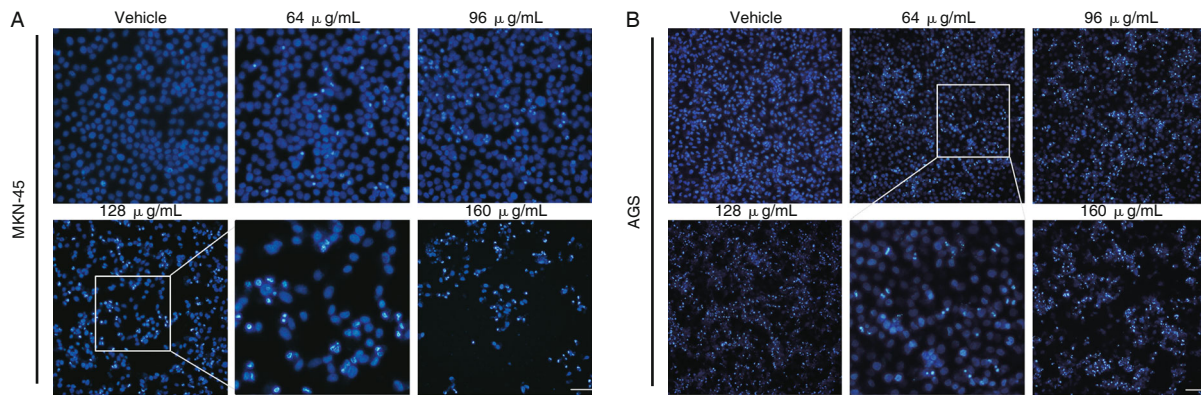
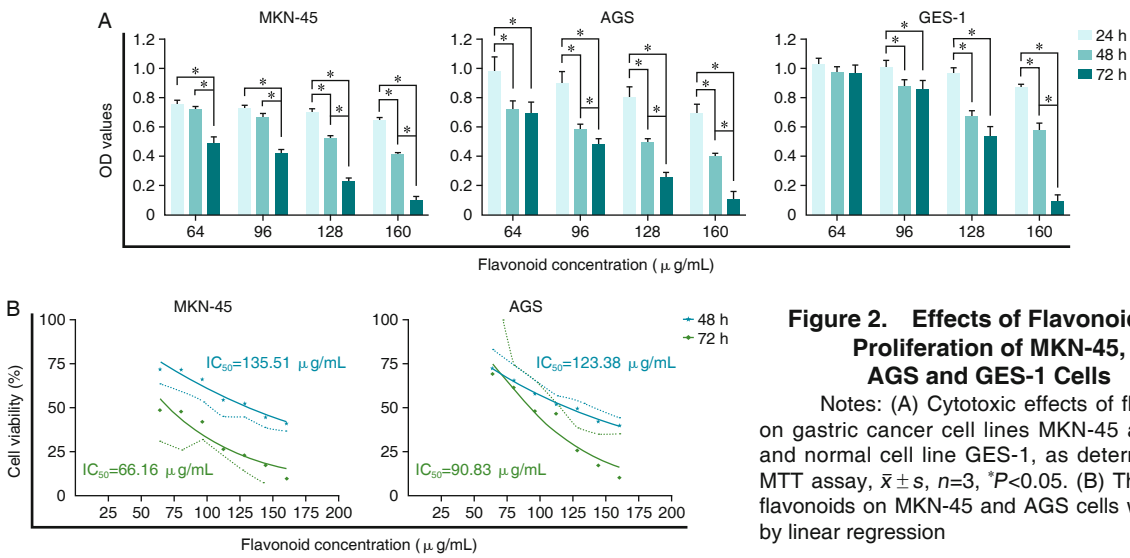


Figure 3. Effects of Flavonoids on Cell Nuclear Morphology of MKN-45 and AGS Cells

Notes: Morphology of MKN-45 and AGS cells visualized with a fluorescence microscope and Hoechst 33342 staining (magnification, $\times 200$) in the vehicle group (RPMI-1640) and flavonoid treatment group. Apoptotic features were assessed by chromatin condensation and fragment staining. Scale bars indicate 200 μm

inhibited proliferation of the MKN-45, AGS cells and GES-1 cells in a time- and dose-dependent manner. The normal gastric mucosal GES-1 cells were not inhibited after 24 h of treatment. The IC_{50} of flavonoids on MKN-45 was 135.51 (48 h) and 66.16 $\mu g/mL$ (72 h). The IC_{50} of flavonoids on AGS were 123.38 (48 h) and 90.83 $\mu g/mL$ (72 h).

Apoptosis of Human Gastric Cancer Cells Induced by Flavonoids

As shown in Figure 3, the nuclei in the vehicle control group were stained uniformly weak blue. In the groups of cells treated with different concentrations of flavonoids, we observed bright blue staining characteristic of cell contraction, chromatin condensation, and nuclear debris; the intensity of staining was dose-dependent.

Compared with the vehicle group (RPMI-1640), after 48 h, as shown in Figure 4 and Appendix 2, the total percent

of apoptosis of the two gastric cancer cell lines increased with increasing flavonoid concentration ($P<0.05$). The early apoptotic cells of MKN-45 rose from 5.1% to 11.6%, the late apoptotic cells increased from 15.2% to 34.3%; the early apoptotic cells of AGS rose from 1.7% to 12.7%, and the late apoptotic cells increased from 18.0% to 28.1%.

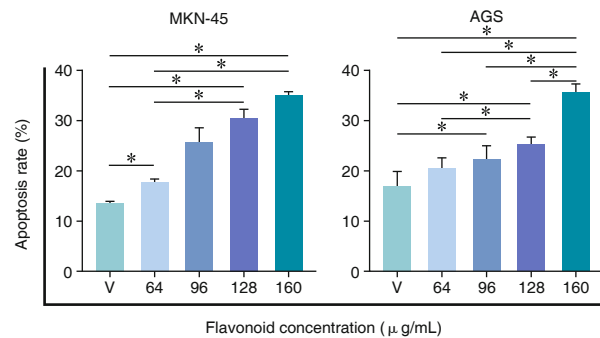


Figure 4. Flavonoids Induce Apoptosis in MKN-45 and AGS Cells ($\bar{x} \pm s$, $n=3$)

Notes: V: vehicle, $*P<0.05$. Cell apoptosis was measured by Annexin V-FITC/PI staining after 48 h

Flavonoids Induced G₁/S Phase Cell Cycle Arrest in Gastric Cancer Cells

PI staining and flow cytometry analysis showed that, compared with the vehicle group (RPMI-1640), the percent of cells in the G₁ phase increased, and the percent of cells in the S phase decreased significantly in a flavonoid dose-dependent manner. As shown in Figure 5 and Appendix 3, the DNA content of MKN-45 cells in G₁ increased from 69.6% to 88.9%, and the DNA content in S phase decreased from 24.2% to 7.8%. The G₁ DNA content of AGS cells increased from 72.0% to 80.6%, and the S phase DNA content decreased from 24.8% to 15.2%. There were significant differences between all treatment groups and the vehicle group ($P < 0.05$). Immunoblotting results showed that flavonoids caused a decrease in Cyclin A and Cdk2 protein levels. Thus, flavonoids successfully induced cell cycle arrest of MKN-45 and AGS cells in G₁/S phase.

Intracellular ROS Production Induced by Flavonoids

As shown in Figure 6, with increasing concentration of flavonoids, the fluorescence intensity increased under a laser confocal microscope. ROS production after NAC (5 mmol/L) pretreatment was lower than that of flavonoids alone, whereas H₂O₂ (1 mmol/L) pretreatment had the opposite effect.

Mitochondrial Pathway of Apoptosis of Gastric Cancer Cells Induced by Flavonoids

As shown in Figure 7, *Oldenlandia diffusa* flavonoids

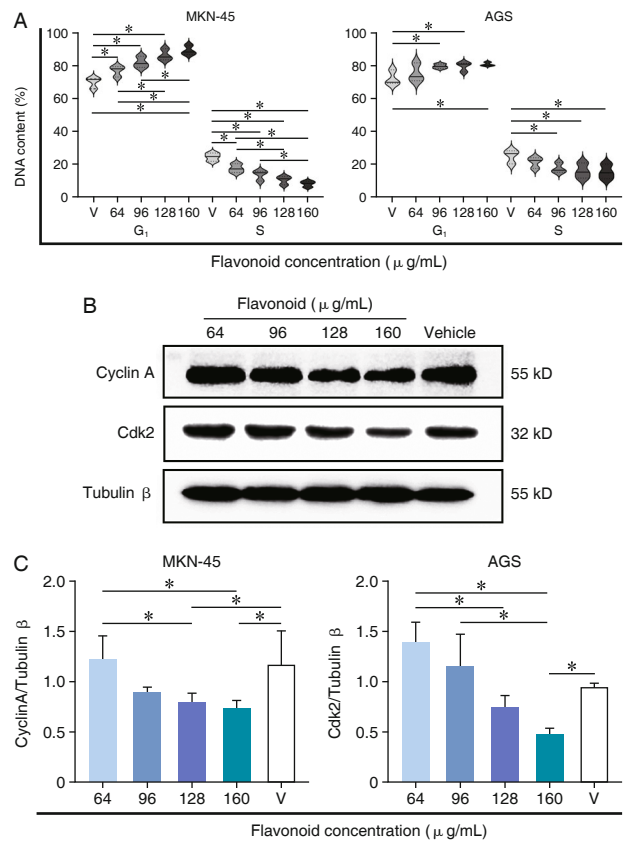


Figure 5. Effects of Flavonoids on Cell Cycle Distribution of MKN-45 and AGS Cells ($\bar{x} \pm s, n=3$)

Notes: (A) Cell cycle distribution of MKN-45 and AGS cells after flavonoids intervention for 48 h determined by PI staining assay, $*P < 0.05$. (B, C) The total protein was extracted from MKN-45, and the expression of cell cycle-related proteins was analyzed by immunoblotting, $*P < 0.05$, V: vehicle

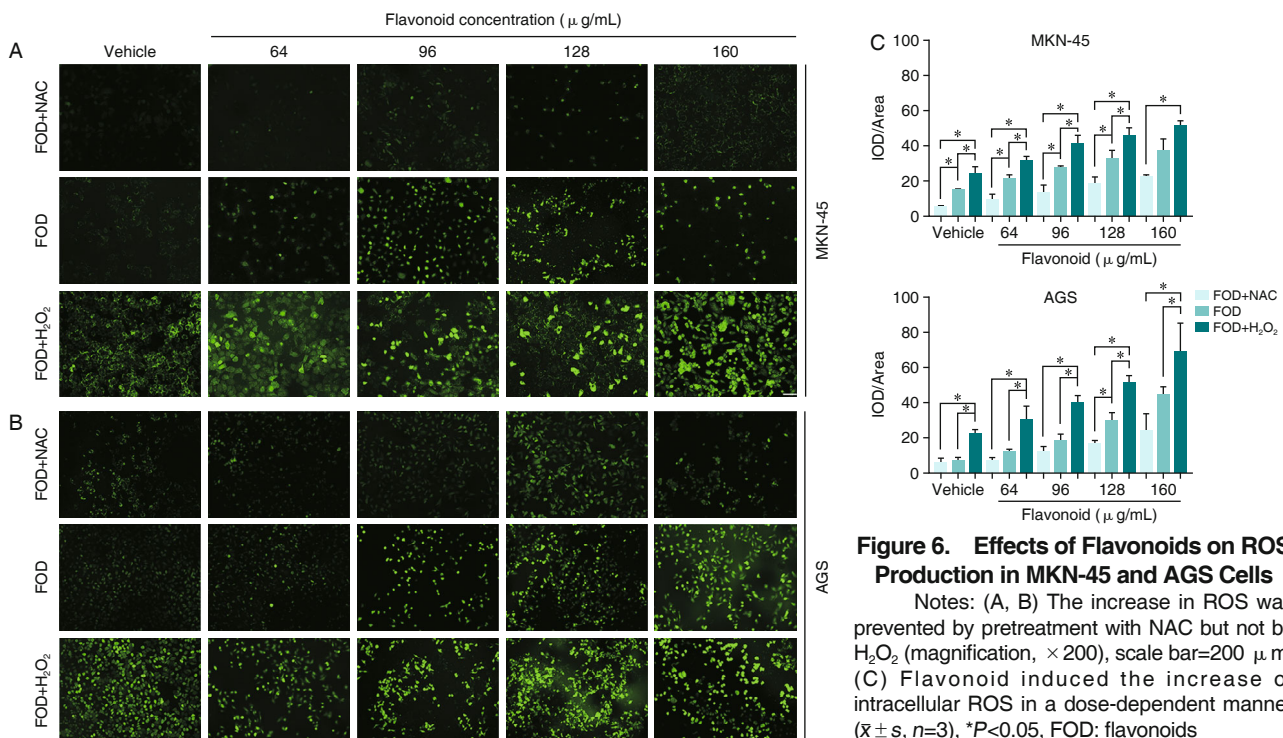


Figure 6. Effects of Flavonoids on ROS Production in MKN-45 and AGS Cells

Notes: (A, B) The increase in ROS was prevented by pretreatment with NAC but not by H₂O₂ (magnification, $\times 200$), scale bar=200 μm. (C) Flavonoid induced the increase of intracellular ROS in a dose-dependent manner ($\bar{x} \pm s, n=3$), $*P < 0.05$, FOD: flavonoids

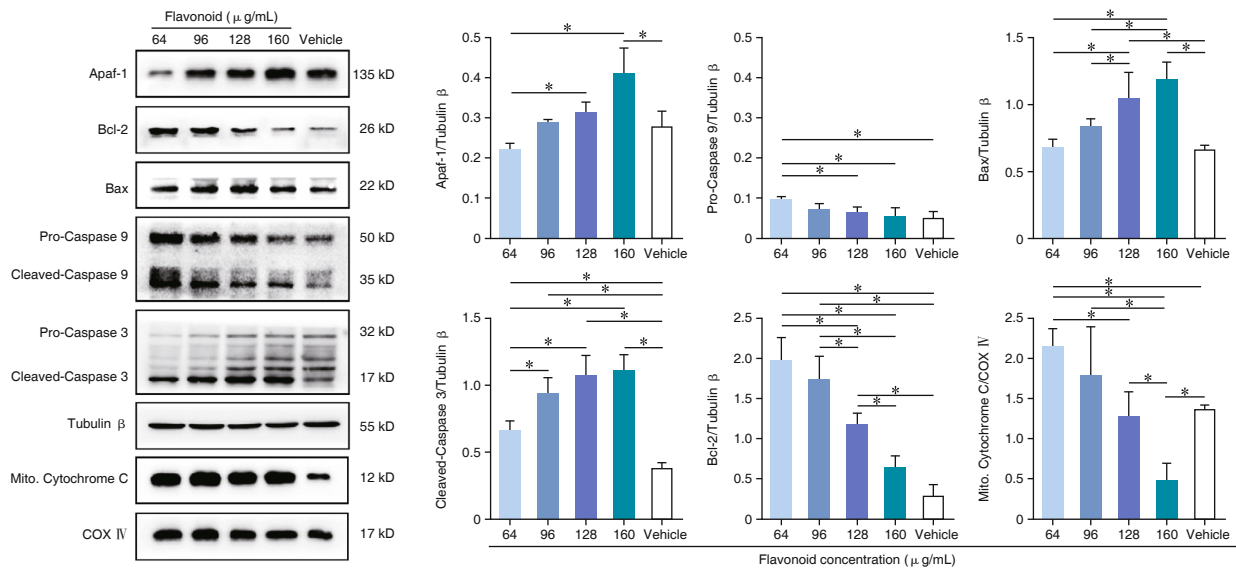


Figure 7. Effects of Flavonoids on Expression of Mitochondrial Apoptotic Proteins by Immunoblotting ($\bar{x} \pm s, n=3$)
 Note: * $P < 0.05$

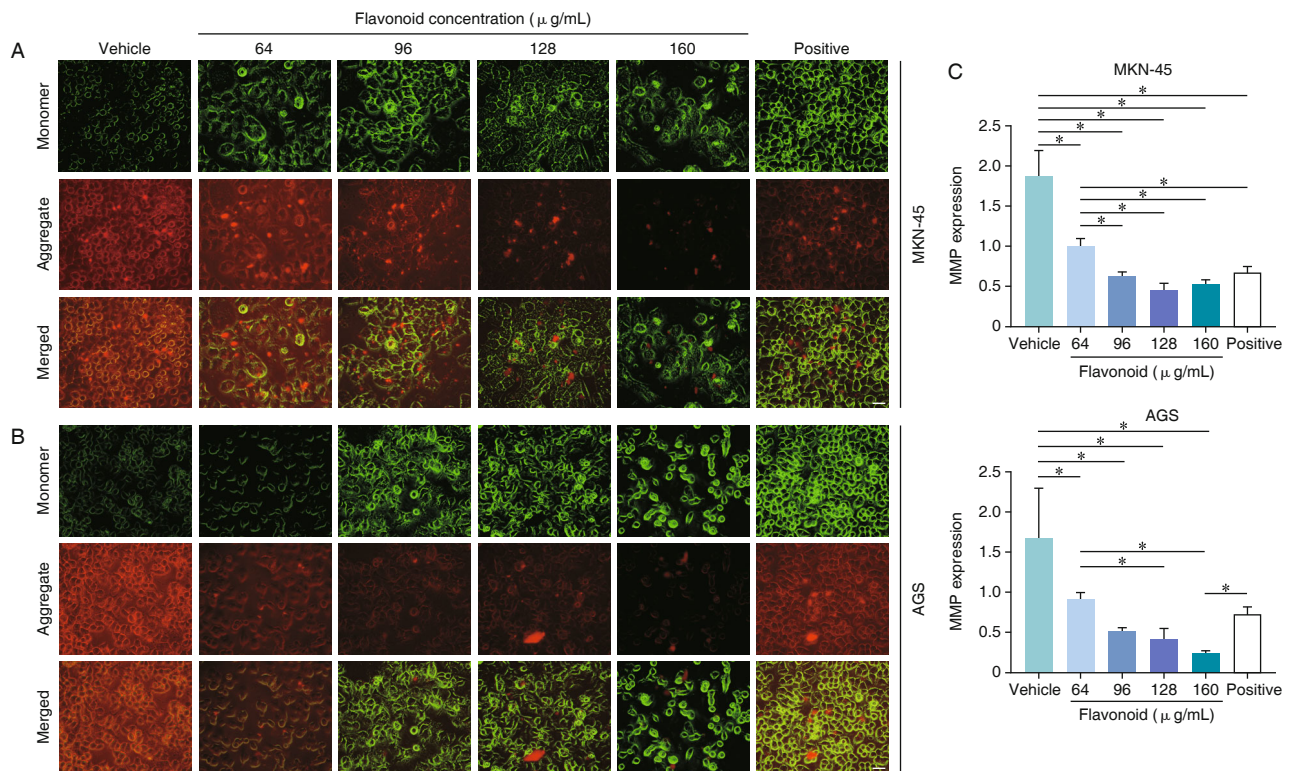


Figure 8. Effects of Flavonoids on MMP Reduction in MKN-45 and AGS Cells

Notes: (A, B) The level of mitochondrial depolarization was observed by fluorescence microscopy (magnification, $\times 400$) and expressed as the red/green fluorescence intensity ratio (Scale bars=50 μm). (C) Bar graphs show that flavonoid induced a disruption of the MMP in a dose-dependent manner ($\bar{x} \pm s, n=3$), * $P < 0.05$

induced expression of apoptotic proteins such as Apaf-1, Cleaved-Caspase-3, and Bax, in a concentration-dependent manner. The expression levels of Pro-Caspase-9 and anti-apoptotic protein Bcl-2 decreased significantly ($P < 0.05$).

As shown in Figure 8, with increasing concentration

of flavonoids, the green fluorescence signal, and the depolarization level of MMP increased. The difference was statistically significant compared with the RPMI-1640 vehicle group ($P < 0.05$). The Cytochrome C in mitochondria decreased with increasing flavonoid concentration. Thus, the flavonoids induced apoptosis mainly through internal

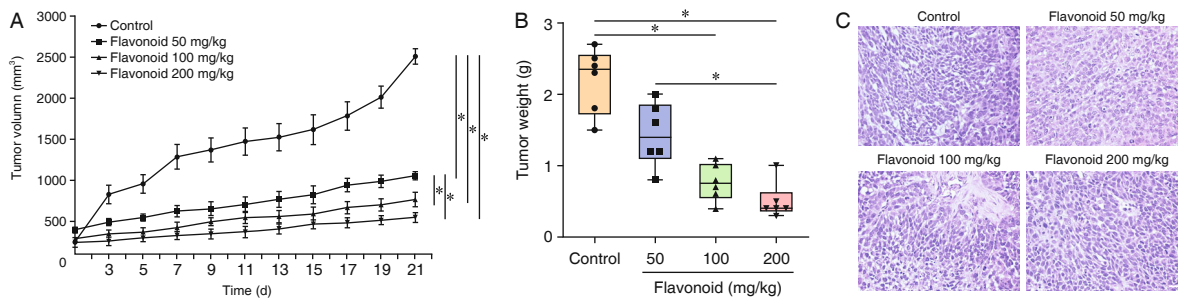


Figure 9. Antitumor Effects of Flavonoids in Xenograft Mice Model

Notes: (A) Tumor volume of each group at different time points ($\bar{x} \pm s$, $n=6$). (B) Final tumor weight of each group assessed at the end of experiment ($\bar{x} \pm s$, $n=6$), $*P<0.05$. (C) Histologic analysis of xenograft tumors evaluated by hematoxylin and eosin staining (magnification, $\times 400$), scale bars= $50 \mu\text{m}$

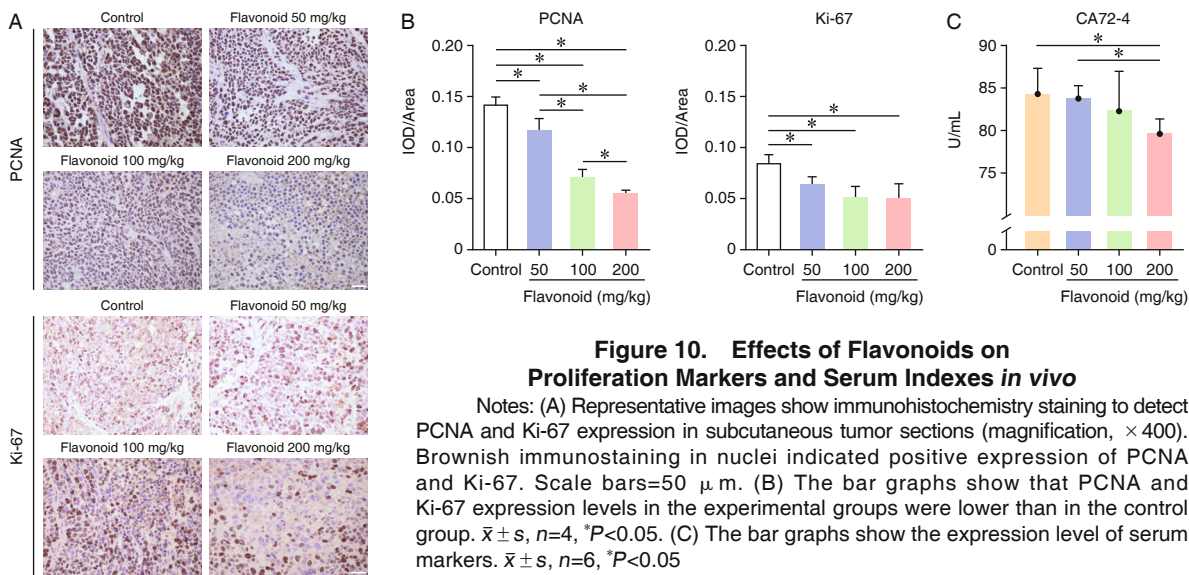


Figure 10. Effects of Flavonoids on Proliferation Markers and Serum Indexes in vivo

Notes: (A) Representative images show immunohistochemistry staining to detect PCNA and Ki-67 expression in subcutaneous tumor sections (magnification, $\times 400$). Brownish immunostaining in nuclei indicated positive expression of PCNA and Ki-67. Scale bars= $50 \mu\text{m}$. (B) The bar graphs show that PCNA and Ki-67 expression levels in the experimental groups were lower than in the control group. $\bar{x} \pm s$, $n=4$, $*P<0.05$. (C) The bar graphs show the expression level of serum markers. $\bar{x} \pm s$, $n=6$, $*P<0.05$

mitochondrial-mediated pathways.

Flavonoids Inhibit Proliferation of MKN-45 Cells in Nude Mice

The tumor weight in the experimental group was less than the weight in the normal saline control group ($P<0.05$, Figures 9A and 9B). There was no significant difference in tumor weight between the high-dose group and the combined-dose group ($P>0.05$). We used HE staining to reveal the subcutaneous tumor tissue. Under the microscope, we observed poorly differentiated, epithelioid, closely arranged tumor cells, and occasionally necrotic areas (Figure 9C).

Immunomodulatory Effect of Flavonoids in Xenograft Model

As shown in Figures 10A and 10B, the protein expression levels in the experimental groups were lower than in the control group. The expression of PCNA and Ki-67 in the high-dose group decreased significantly ($P<0.05$). These results showed that *Oldenlandia diffusa*

flavonoids inhibited the proliferation of MKN-45 cells in nude mice. As shown in Figure 10C, the expression level tumor marker CA72-4 was lower than those in the control group ($P<0.05$).

DISCUSSION

In this study, we evaluated the ability of *Oldenlandia diffusa* flavonoids at different concentrations to induce apoptosis of human gastric cancer cells MKN-45 and AGS. We found that flavonoids inhibited proliferation and induced apoptosis in a dose- and time-dependent manner. In addition, after intervention of total flavonoids, the production of ROS in tumor cells, the depolarization level of MMP, and the expression level of critical apoptotic proteins increased, which suggested that flavonoids had a key activity in the mitochondrial-mediated apoptosis signal pathway.

The mitochondrial membrane is the primary source of ROS.⁽²⁰⁾ Cell damage depends on not only the intracellular concentration of ROS, but also the generation of oxidative stress during oxidation/

antioxidant imbalance.⁽²¹⁾ This phenomenon will directly lead to the destruction of mitochondrial electron transfer and energy metabolism, activate and release apoptosis-related proteins, and finally change the cell redox potential to cause apoptosis.⁽²²⁾ Our results emphasize the importance of ROS accumulation and unbalanced oxidation leading to the loss of MMP in the resistance of flavonoids to the proliferation of gastric cancer cells.

Oxidative stress activates the DNA damage response, which, in turn, causes cell cycle arrest. Most tumor cells undergo programmed cell death in the form of apoptosis.⁽²³⁾ The flavonoids blocked the cell cycle in G₁/S phase. Considering that the reason for flavonoid-induced arrest of the cell cycle was related to the obstruction of DNA synthesis, we turned our attention to the effect on cell cycle-related proteins. We found decreased expression of Cyclin A and Cdk2 that regulate the G₁/S phase transition. Hwang, et al⁽²⁴⁾ showed that calming cells (G₀) activated Cyclin A and Cdk2 to start DNA synthesis under mitotic stimulation. When this process was inhibited, the cell cycle stagnated in G₁/S phase; our results were consistent with this finding. In addition, Mansilla, et al⁽²⁵⁾ found that inhibition of CDK protein by p21 triggered cell cycle arrest in S phase; this function of p21 depended entirely on its ability to replace chromatin and bind PCNA. The activity of PCNA is positively correlated with the DNA content of S phase cells. To further evaluate the cell proliferation activity, we focused on Ki-67 and PCNA, two proteins commonly used to detect and quantify proliferating cells.^(25,26) We observed that expression of PCNA and Ki-67 also decreased in mouse tumor tissues. The results showed that the flavonoid affected the mitotic process by blocking the G₁/S phase of the cell cycle.

The key factor in the initiation of the mitochondrial apoptosis pathway is the release of death effector Cytochrome C. We found that Cytochrome C abundance decreased with increasing concentrations of *Oldenlandia diffusa* flavonoids. This finding indicated that increasingly more Cytochrome C was released from mitochondria into the cytoplasm, it bound to Apaf-1, formed an activation complex with Caspase-9, which then Cleaved-Caspase-3 to trigger caspase-dependent signal transduction. In addition, the Bcl-2 protein family regulates apoptosis by controlling MMP.⁽²⁷⁾ We found that the expression of pro-apoptotic protein Bax increased, and the presentation of Bcl-2 in the mitochondrial outer membrane decreased. These results suggested that the flavonoids further triggered activation of the mitochondrial signal pathway

through the caspase-dependent signal pathway to induce apoptosis of the gastric cancer cells.

In summary, studies *in vivo* and *in vitro* showed that *Oldenlandia diffusa* flavonoids inhibited proliferation of human gastric cancer cell lines MKN-45 and AGS, blocked the cell cycle in the G₁/S phase, and induced apoptosis by intracellular ROS accumulation, loss of MMP, and activation of mitochondrial pathway. *Oldenlandia diffusa* flavonoids can inhibit tumor growth in mice, reduce the level of proliferation markers and tumor markers. Although we used only MKN-45 cells to verify the mitochondrial apoptosis pathway-related proteins and the reliability of the current conclusions on tumor tissues are not further investigated, we suggest that it is of great significance to investigate the mechanism of *Oldenlandia diffusa* flavonoids inhibition of gastric cancer.

Conflict of Interest

The authors declare no conflict of interest.

Author Contributions

Wang QL designed the study and guided the revision of the manuscript. Ling JY completed most of the experimental projects and wrote the manuscript. Yin DH assisted Ling JY in animal feeding and provided technical guidance for animal experiments. Lin L instructed Liang HN and Liu QB regarding flavonoid extraction. All authors read and approved the final version.

Electronic Supplementary Material: Supplementary material (Appendices 1–3) is available in the online version of this article at <https://doi.org/10.1007/s11655-022-3679-4>.

REFERENCES

1. Machlowska J, Baj J, Sitarz M, Maciejewski R, Sitarz R. Gastric cancer: epidemiology, risk factors, classification, genomic characteristics and treatment strategies. *Int J Mol Sci* 2020;21:4012.
2. Ferlay J, Shin HR, Bray F, Forman D, Mathers C, Parkin DM. Estimates of worldwide burden of cancer in 2008: GLOBOCAN 2008. *Int J Cancer* 2010;127:2893-2917.
3. Slagter AE, Vollebergh MA, Jansen EPM, Sandick JW, Cats A, Grieken NCT, et al. Towards personalization in the curative treatment of gastric cancer. *Front Oncol* 2020;10:614907.
4. Wagner AD, Syn NL, Moehler M, Grothe W, Yong WP, Tai BC, et al. Chemotherapy for advanced gastric cancer. *Cochrane Database Syst Rev* 2017;8:CD004064.
5. Huang WJ, Ruan S, Wen F, Lu XN, Gu SP, Chen XX, et al. Multidrug resistance of gastric cancer: the mechanisms

- and chinese medicine reversal agents. *Cancer Manag Res* 2020;12:12385-12394.
6. Cheng YY, Hsieh CH, Tsai TH. Concurrent administration of anticancer chemotherapy drug and herbal medicine on the perspective of pharmacokinetics. *J Food Drug Anal* 2018;26:S88-S95.
 7. Chen R, He JY, Tong XL, Tang L, Liu MH. The *Hedyotis diffusa* Willd. (Rubiaceae): a review on phytochemistry, pharmacology, quality control and pharmacokinetics. *Molecules* 2016;21:710.
 8. Hu CJ, He J, Li GZ, Fang PP, Xie JD, Ding YW, et al. Analyzing *Hedyotis diffusa* mechanisms of action from the genomics perspective. *Comput Methods Programs Biomed* 2019;174:1-8.
 9. Huo JY, Lu Y, Jiao YK, Chen DF. Structural characterization and anticomplement activity of an acidic polysaccharide from *Hedyotis diffusa*. *Int J Biol Macromol* 2020;155:1553-1560.
 10. Zhang Y, Xie RF, Xiao QG, Li R, Shen XL, Zhu XG. *Hedyotis diffusa* Willd extract inhibits the growth of human glioblastoma cells by inducing mitochondrial apoptosis via AKT/ERK pathways. *J Ethnopharmacol* 2014;158:404-411.
 11. Hu EP, Wang DG, Chen JY, Tao XL. Novel cyclotides from *Hedyotis diffusa* induce apoptosis and inhibit proliferation and migration of prostate cancer cells. *Int J Clin Exp Med* 2015;8:4059-4065.
 12. Zhang PY, Zhang B, Gu J, Hao L, Hu FF, Han CH. The study of the effect of *Hedyotis diffusa* on the proliferation and the apoptosis of the cervical tumor in nude mouse model. *Cell Biochem Biophys* 2015;72:783-789.
 13. Li YL, Zhang JL, Min D, Zhou HY, Lin N, Li QS. Anticancer effects of 1,3-dihydroxy-2-methylanthraquinone and the ethyl acetate fraction of *Hedyotis Diffusa* Willd against HepG2 carcinoma cells mediated via apoptosis. *PLoS One* 2016;11:e0151502.
 14. Lin LY, Cheng KL, Xie ZQ, Chen CY, Chen L, Huang YD, et al. Purification and characterization a polysaccharide from *Hedyotis diffusa* and its apoptosis inducing activity toward human lung cancer cell line A549. *Int J Biol Macromol* 2019;122:64-71.
 15. Wang QL, Xue YJ, Han T. Extraction of flavone in *Hedyotis diffusa* Wild and its effect on gastric cancer cell BGC-823 in proliferation cycle and apoptosis. *Chin J Integr Tradit West Med Dig (Chin)* 2015;23:760-763.
 16. Liang HN, Liu QB, Ling JY, Lin L, Liu JN, Wang X, et al. Extraction of flavonoids from *Oldenlandia diffusa* by enzymatic-ultrasonic assisted method. *Chin Pharm J (Chin)* 2021;56:1041-1047.
 17. Wang X, Xia SL, Liu JN, Ling JY, Wang QL, Lin L, et al. Study on purification process of total flavonoids from *Oldenlandia diffusa* by macroporous resin and its tumor inhibition *in vivo*. *Inf Tradit Chin Med (Chin)* 2021;38:16-21.
 18. Li M, Zhang HY, Shao HO. Effects of total flavonoids of *Oldenlandia diffusa* on immunity and antioxidant capacity of cervical cancer U14 bearing mice. *J Chin Med Mater (Chin)* 2019;42:1417-1420.
 19. Wang X, Ling JY, Zhai YC, Xia SL, Wang QL, Han T. Effects of total flavonoids of *Oldenlandia diffusa* on serum tumor markers and immune function of MFC gastric cancer bearing mice. *Chin J Clin Pharmacol (Chin)* 2021;37:2627-2630.
 20. Ruth SS, Elazar Z. Regulation of autophagy by ROS: physiology and pathology. *Trends Biochem Sci* 2011;36:30-38.
 21. Sosa V, Moliné T, Somoza R, Paciucci R, Kondoh H, LLeonart ME. Oxidative stress and cancer: an overview. *Ageing Res Rev* 2013;12:376-390.
 22. Li ZY, Yang Y, Ming M, Liu B. Mitochondrial ROS generation for regulation of autophagic pathways in cancer. *Biochem Biophys Res Commun* 2011;414:5-8.
 23. Kuczler MD, Olseen AM, Pienta KJ, Amend SR. ROS-induced cell cycle arrest as a mechanism of resistance in polyaneploid cancer cells (PACCs). *Prog Biophys Mol Biol* 2021;165:3-7.
 24. Hwang CY, Lee SM, Park SS, Kwon KS. CDK2 differentially controls normal cell senescence and cancer cell proliferation upon exposure to reactive oxygen species. *Biochem Biophys Res Commun* 2012;425:94-99.
 25. Mansilla SF, Vega MB, Calzetta NL, Siri SO, Gottifredi V. CDK-independent and PCNA-dependent functions of p21 in DNA replication. *Genes (Basel)* 2020;11:593.
 26. Zambon AC. Use of the Ki67 promoter to label cell cycle entry in living cells. *Cytometry A* 2010;77:564-570.
 27. Wang J, Deng HY, Zhang JX, Wu DD, Li J, Ma JJ, et al. α -Hederin induces the apoptosis of gastric cancer cells accompanied by glutathione decrement and reactive oxygen species generation via activating mitochondrial dependent pathway. *Phytother Res* 2020;34:601-611.

(Accepted April 25, 2022; First Online August 31, 2022)

Edited by YUAN Lin